Laboratory Investigation (2010) 90, 1805–1816

Kupffer cells are associated with apoptosis, inflammation and fibrotic effects in hepatic fibrosis in rats

Cheng Liu[1,2], Qing Tao[1], Mingyu Sun[1], Jim Z Wu[3], Wengang Yang[3], Ping Jian[1], Jinghua Peng[1], Yiyang Hu[1], Chenghai Liu[1,*] and Ping Liu[2,4,*]

Hepatocellular apoptosis, hepatic inflammation, and fibrosis are prominent features in chronic liver diseases. However, the linkage among these processes remains mechanistically unclear. In this study, we examined the apoptosis and activation of Kupffer cells (KCs) as well as their pathophysiological involvement in liver fibrosis process. Hepatic fibrosis was induced in rats by dimethylnitrosamine (DMN) or carbon tetrachloride (CCl4) treatment. KCs were isolated from normal rats and incubated with lipopolysaccharide (LPS) or from fibrotic rats. The KCs were stained immunohistochemically with anti-CD68 antibody, a biomarker for KC. The level of expression of CD68 was analyzed by western blot and real-time PCR methods. The apoptosis and pathophysiological involvement of KCs in the formation of liver fibrosis were studied using confocal microscopy. The mRNA and protein expression of CD68 were significantly increased in DMN- and CCL4-treated rats. Confocal microscopy analysis showed that CD68-positive KCs, but not α-smooth muscle actin (SMA)-positive cells, underwent apoptosis in the liver of DMN- and CCL4-treated rats. It was also revealed that the terminal deoxynucleotidyl transferase-mediated dUTP nick-end labeling and CD68-double-positive apoptotic KCs located in the portal or fibrotic septa area were situated next to hepatic stellate cells (HSCs). Tumor necrosis factor-α (TNF-α) and KC co-localized in the liver in the neighbor of HSCs. The double α-SMA- and collagen type I-positive cells predominantly existed in fibrotic septa, and those cells were co-localized clearly with CD68-positive cells. Interestingly, some CD68 and Col (1) double positive, but completely negative for α-SMA, were found in the portal areas and hepatic sinusoids; this phenomenon was also validated in primary isolated KCs after 6 h LPS exposure or fibrotic rats *in vitro*. These results show that KCs are associated with hepatocellular apoptosis, inflammation, and fibrosis process in a liver fibrosis models.

Laboratory Investigation (2010) **90,** 1805–1816; doi:10.1038/labinvest.2010.123; published online 4 October 2010

KEYWORDS: apoptosis; hepatic stellate cell; inflammation; Kupffer cell; liver fibrosis

Over the past 10–15 years, our understanding about the pathogenesis of human liver fibrosis has progressed significantly.[1–3] This dramatic change in our understanding of liver fibrosis evolved over time beginning with the study of matrix biology, which led to hepatic stellate cells (HSCs) biology, and finally progressed to the current era of 'the integrated wound healing response'.[4] Indeed, evidence suggests that the microenvironment *in vivo* has an important function in regulating HSC activation and function.[5] Among the complex microenvironment factors, Kupffer cells (KCs), or the resident hepatic macrophages, carry out an important function in modulating inflammation in liver fibrosis development.[6–9] In the case of liver fibrosis, it has been suggested that KCs produce a variety of proinflammatory cytokines such as tumor necrosis factor-α (TNF-α) and monocyte chemoattractant protein that provokes the activation of HSCs, which produces extracellular matrix protein, in particular collagen I, and subsequently contribute to hepatic injury.[10,11]

Recently, hepatocellular apoptosis was found to have a pivotal function in liver fibrogenesis.[12] These apoptotic

[1]Institute of Liver Diseases, Shuguang Hospital, Shanghai, People's Republic of China; [2]Shanghai University of Traditional Chinese Medicine, Shanghai, People's Republic of China; [3]Roche R&D Center (China), Shanghai, People's Republic of China and [4]E-institute of Shanghai Municipal Education Commission, Shanghai, People's Republic of China

*Correspondence: Professor P Liu or Professor C Liu, Shanghai University of Traditional Chinese Medicine, 1200 Cailun Road, Shanghai 201203, People's Republic of China.

E-mail: liuliver@vip.sina.com

Received 19 October 2009; revised 19 April 2010; accepted 5 May 2010

events are associated with chronic liver diseases and are increasingly viewed as a nexus of liver injury and fibrosis.[13] However, the detailed relationship between apoptosis and either hepatic inflammation or fibrosis has not been fully explored. Various studies have shown that KCs might act as an integral factor in these serial pathogenic events. It was reported that KCs engulf apoptotic bodies originated from hepatocytes, erythrocytes, and neutrophils. This event accelerates liver inflammation and fibrosis.[14–16] To date, the secretion of proinflammatory cytokines and modulation of HSC activity by KCs have only been documented in *in vitro* cell cultures, but not in any *in vivo* system.[17] Nevertheless, there is mounting evidence suggesting that KCs are involved in pathophysiology of liver injury resolution *in vivo*.[18]

It has been shown that acute, high dosing of dimethylnitrosamine (DMN) induced a massive hepatocellular apoptosis that may contribute to liver toxicity.[19] However, apoptosis was rarely reported as a result of long-term low-dose DMN exposure. We recently showed that α-smooth muscle actin (α-SMA)-positive HSC apoptosis was not frequently observed in DMN-induced liver fibrosis.[20]

Here, we seek to ascertain the functional status of KCs and show the pathophysiological involvements of KCs in DMN and carbon tetrachloride (CCL4)-induced liver fibrosis *in vivo* through a detailed confocal laser microscopy study. We discovered evidences that a portion of KCs might undergo apoptosis in DMN- and CCL4-treated liver and that KCs might activate HSCs by secreting TNF-α and/or directly interacting with HSCs. Finally, besides activated HSCs, KCs acted as an alternative resource for collagen I production. These findings benefit our understanding of important mechanisms of KCs and potential linkage among apoptosis, inflammation, and fibrosis in liver injury.

MATERIALS AND METHODS

Reagents

DMN and CCL4 were purchased from Sigma (Saint Louis, MO, USA). Sirius red was obtained from Polysciences (09400-25, Warrington, PA USA). SYBR Green Supermix was from Takara (Ostu, Shiga, Japan). Latex beads, polystyrene (LB8), collagenase (C5138) from *Clostridium histolyticum*, and lipopolysaccharide (LPS) (L2880) from *Escherichia coli* serotype 055:B5 were purchased from Sigma-Alrich (Saint Louis, MO, USA). Nycodenz was purchased from Nycomed Pharma AS, Oslo, Norway. DNase I (11284932001) from bovine pancreas lyophilized sterile filtered, Pronase (11459643001) from *Streptomyces griseus* were purchased from Roche Diagnostics GmbH (Mannheim, Germany). Dulbecco's modified Eagle medium (DMEM, 12100-046), minimum essential medium (41500-034), and fetal calf serum (FCS, 10437010) were purchased from Gibco Invitrogen (Grand Island, NY, USA). Prestained protein marker was purchased from New England Biolabs (Beijing, China). ApopTag Fluorescein *In Situ* Apoptosis Detection kit (S7110) was purchased from Chemicon (Temecula, CA, USA). For the primary antibodies used in immunostaining and western blot, anti-Fas mouse antibody was purchased from BD Pharmingen and used in 1:1000 dilution, and anti-CD68 mouse antibody was purchased from Serotec and prepared in 1:100 dilution. Anti-TNF-α rabbit antibody was purchased from Chemicon and diluted to 0.2 μg/ml. Anti-collagen type I (col1) rabbit antibody was purchased from Calbiochem and used in 1:100 dilution. Anti-α-SMA mouse antibody was from Sigma and diluted in 1:400 ratio. Anti-FasL (ab15285) rabbit antibody was purchased from Abcam and used in 1:100 dilution. Anti-glyceraldehyde 3-phosphate dehydrogenase mouse antibody was purchased from Kangchen and diluted in 1:5000 ratio. Secondary fluorescence-labeling goat anti-mouse FITC, Cy3 antibody were obtained from Jackson (West Grove, PA, USA) and used in 1:1000 dilution. Labeled goat anti-mouse isotype-specific antibody Alexa Fluor 647 immunoglobulin G $(IgG)_{2a}$ was from Molecular Probes (MD, USA) and used at 5 μg/ml.

Liver Injury Models

Male Spragus–Dawley rats at 180–200 g were housed in an air-conditioned room at 25°C with a 12 h darkness/light cycle. The rats received humane care with unlimited accesses to chow food and water during the study. All of this study's protocols comply with the current ethical considerations of Shanghai University of Traditional Chinese Medicine's Animal Ethic Committee.

For DMN-induced liver fibrosis model, the rats were randomized into two groups: control ($n=10$) and DMN treated ($n=18$). DMN (10 mg/kg) was administered intraperitoneally for 3 consecutive days each week for 2 or 4 weeks.[21] Control rats received equal quantities of physiological saline. At the end of the second week, three rats from the control and six rats from the DMN-treated group were killed to assess fibrosis development. At the end of the fourth week, all of the animals were killed and their liver samples were collected for histology and immunochemistry analyses.

For CCL4-induced liver fibrosis, the rats were randomized into two groups: control ($n=10$) and CCL4 treated (18). CCL4 (2 ml/kg) was administered intraperitoneally twice weekly for 6 or 9 weeks.[22] At the end of the sixth week, three rats from the control and six rats from the CCL4-treated group were killed for fibrosis development assessment; at the end of the ninth week, all of the animals were killed.

Liver Histology

Liver specimens were preserved in 4% paraformaldehyde and dehydrated in a graded alcohol series. Specimens were then embedded in paraffin blocks, cut into 5 μm-thick sections, and placed on glass slides. Sections were then stained with Sirius red by a normal procedure.

Hepatic Hydroxyproline Content

Liver tissue (100 mg) was prepared for hydroxyproline (Hyp) determination according to a modification of method by

Jamall *et al.*[23] The Hyp content of the liver as an indirect measure of tissue collagen content was expressed in microgram per gram of wet weight (μg/g).

Immunohistochemical Staining

After deparaffinization and dehydration, microwave antigen retrieval was performed for 5 min before peroxidase quenching with 3% H_2O_2 in phosphate-buffered saline (PBS) for 15 min. Subsequently, the sections were blocked with 5% bovine serum albumin (BSA) for 30 min and then incubated, respectively, with the primary antibodies (anti-α-SMA, anti-CD68, and anti-Fas antibody) overnight at 4°C with a dilution ratio of 1:100 in PBS. Negative control was treated the same as sample groups except the primary antibodies were omitted in the incubation. After washed in PBS, sections were then incubated with biotinylated secondary antibodies for 30 min and then stained with 3, 3′-diaminobenzidine (Vector, Burlingame, CA, USA) for 2–5 min. Slides were counterstained with hematoxylin for 2–3 min, mounted, and examined.

Laser Confocal Microscopy

Liver samples were assessed grossly and immersed immediately into cyromatrix (Tissue-Tek OCT, Sakura Finetek, Torrance, CA, USA) and snap frozen in liquid nitrogen; 5 μm sections were cut. Terminal deoxynucleotidyl transferase-mediated dUTP nick-end-labeling (TUNEL) assay was performed using a commercially available kit (Chemicon) following the manufacturer's instructions. Thereafter, the slides were incubated with 5% BSA for 30 min and followed by incubation with anti-CD68 primary antibody at 37°C for 1 h. Slides were then washed three times with PBS and incubated with the secondary Cy3-conjugated affinipure goat anti-mouse antibody for 30 min.

Tri-color immunofluorescence staining was performed on cryosections by using different combinations of antibodies. For instance, in the tri-color labeling of TUNEL, CD68, and α-SMA, liver sections were first performed for TUNEL by following the manufacture's introductions. Then liver sections were incubated with monoclonal anti-CD68 for 1 h at room temperature. Biotin-conjugated anti-mouse IgG1 was then added and incubated for 30 min. The staining reaction was developed with Cy3-conjugated streptavidin for 30 min. After washing, the sections were incubated with α-SMA antibody followed by Alexa Fluor 647-labeled goat anti-mouse isotype-specific antibody and then covered with mounting medium. Imaging analyses were performed using a Leica (Mannheim, Germany) DMIRBE inverted stand and Leica TCS2MP confocal system.

Western Blot Analysis

Liver samples were prepared in radio immunoprecipitation lysis buffer containing protease inhibitors. After protein quantification, protein samples at 50 μg/lane were subjected to polyacrylamide gel electrophoresis and transferred to Immobilon-P transfer membranes, which were then blocked and exposed to the respective antibodies. Bound antibodies were visualized using an enhanced chemiluminescence kit (Pierce, Rockford, IL, USA) and exposed to Kodak BioMax film (Kodak, Rochester, NY, USA).

RNA Isolation and Gene Expression Analysis

Total RNA ($\sim$50 mg) from liver tissue was isolated using Trizol reagent (Invitrogen, Carlsbad, CA, USA). cDNA synthesis was performed using 4 μg of total RNA per sample with random primers and reagents contained in the RevertAid First Strand cDNA Synthesis kit according to the manufacture's protocol (Fermentas, Glen Burnie, MD, USA). The reverse transcriptase product was 10-fold diluted in nuclease-free H_2O. In total, 2 μl of each sample was loaded into 36-well tubes for real-time PCR in a Rotor-gene 3000 (Corbett Research, Sydney, NSM, Australia). The 18S rRNA served as internal controls. Relative quantization was calculated using the delta–delta cycle threshold method. Sequences and the accession numbers of the primers for real-time PCR of CD68 (Gene Bank Accession No. NM001031638) were 5′-TGTACCTGACCCAGGGTGGAA-3′ (forward primer) and 5′-GAATCCAAAGGTAAGCTGTCCGTAA-3′ (reverse primer) with a predicted length of 140 bp of amplified product. For TNF-α (Gene Bank Accession No. X6659), the forward primer was 5′-GGCAGCCTTGTCCCTTGA- AGAG-3′ and the reverse primer 5′-GTAGCCCACGTCGTAGCAAACC-3′ with a predicted length of 171 bp of amplified product. For col1(α1) (Gene Bank Accession No. NM_007742), the forward primer was 5′-ACTCAGCCGTCTGTGCCTCA-3′ and the reverse primer 5′-GGAGGCCTCGGTGGACATTA-3 with a length of 187 bp. For 18S rRNA (Gene Bank Accession No. X0117), the forward primer sequence was 5′-GTAACCCGTTGAACCCCA TT-3′ and reverse was 5′-CCATCCAATCGGTAGTAGCG-3′ with a length of 151 bp of amplified product.

Primary KCs Isolation and Culture

KCs were isolated from normal male Wastar or fibrotic rats induced by DMN for 2 weeks by sequential pronase/collagenase perfusion. After anesthesia and abdominal exploration, the liver was perfused through the portal vein with 50 ml Gey's balanced salt solution (GBSS). Perfusion was followed by 200 ml of GBSS containing 120 mg pronase and 17 mg collagenase. The liver was removed and cut into small pieces, which were then incubated at 37°C for 30 min in GBSS solution containing 1 mg/ml pronase and 0.2 mg/ml DNase. The resulting suspension was filtered through a 150 mm steel mesh. Hepatocytes were then removed by centrifugation. The supernatant was saved and the isolation of KCs was achieved by a density gradient centrifugation with Nycodenz (9.5% over 14.5%) at 1400 *g*, 25°C, for 22 min, which produced a KC-enriched fraction in the middle whitish layer. Purification was achieved by allowing the cells to adhere to plastic culture plates at 37°C for 20 min, nonadherent cells were removed by washing. The viability of cells

was always >95% as determined by trypan blue exclusion. Cells were plated in six-well plastic culture dishes (Corning, NY, USA) at a concentration of 4×10^6 cells/well and were cultured in DMEM containing 20% FCS at 37°C in a humidified atmosphere of 5% CO_2 for 48 h for further studies. Purity of the KC culture, determined by latex beads staining, was routinely >95%. This purity was further confirmed with the immunostaining with antibodies against CD31 (marker of endothelial cells) and α-SMA (marker of HSCs) to exclude non-KCs contaminations.

The medium was removed and cells were carefully washed with PBS three times, then 2 ml of media containing either vehicle (saline) or LPS at a final concentration of 100 μg/l was added to each well. Samples were taken from the medium for 6 h after incubation at 37°C for Col (1) RNA analyses through real-time PCR.

To extract RNA from KC, cultured KCs were washed with ice-cold PBS and lyzed, then total RNA was isolated using the RNeasy mini kit (Qiagen) as per the manufacturer's instructions. RNA was then treated with 1 μl RNA-qualified ribonuclease-free deoxyribonuclease I (1U/μl; Promega) per 1 μg total RNA for 30 min at 37°C to ensure complete removal of DNA contamination.

For immuncytochemistry, freshly isolated KCs were cultured on eight wells Lab-Tek chamber slides (Nunc, Naperville, IL, USA). KCs isolated from control rats were cultured for 48 h, followed with a 6-h LPS stimulation. Those cells were then used for confocal microscopy study. After isolation, the freshly prepared KCs from fibrotic rats were used for confocal microscopy detection.

Statistical Analysis

Each experiment was performed at least three independent times. All the results are expressed as mean ± s.d. Statistical test was performed with SPSS software version 11.5. Groups were compared using one-way analysis of variance with Dunnett's multiple comparison test or the student-Newman–Keuls test (where applicable). $P<0.05$ was considered statistically significant.

RESULTS

Liver Fibrosis Induced by DMN and CCL4

Liver fibrosis in rats after administration of DMN and CCL4 was confirmed by several lines of evidences. First, the accumulation of an extracellular matrix, especially the collagen, was clearly revealed by Sirius red. As shown in Figure 1A and Supplementary Figure 1a, collagen staining was scarcely observed in the control liver samples except the area around small central venous walls. In DMN-treated liver samples at 2 weeks, collagen was seen to stretches from portal area to lobular (Figure 1B). In 6-week CCL4-treated rats, incomplete septa were also noticed (Supplementary Figure 1b). Additional cirrhotic nodule formation was visualized in 4-week DMN-treated or 9-week CCL4-treated rats (Figure 1C; Supplementary Figure 1c). To evaluate the progression of fibrosis in a quantitative manner, liver Hyp content was measured. After 2-week DMN administration, the Hyp content was ~161% of that in the control group ($P<0.01$) (Figure 1b). The increase reached at 360% ($P<0.01$) in 4-week DMN-treated liver samples when compared with the control, which coincided with the progression of marked

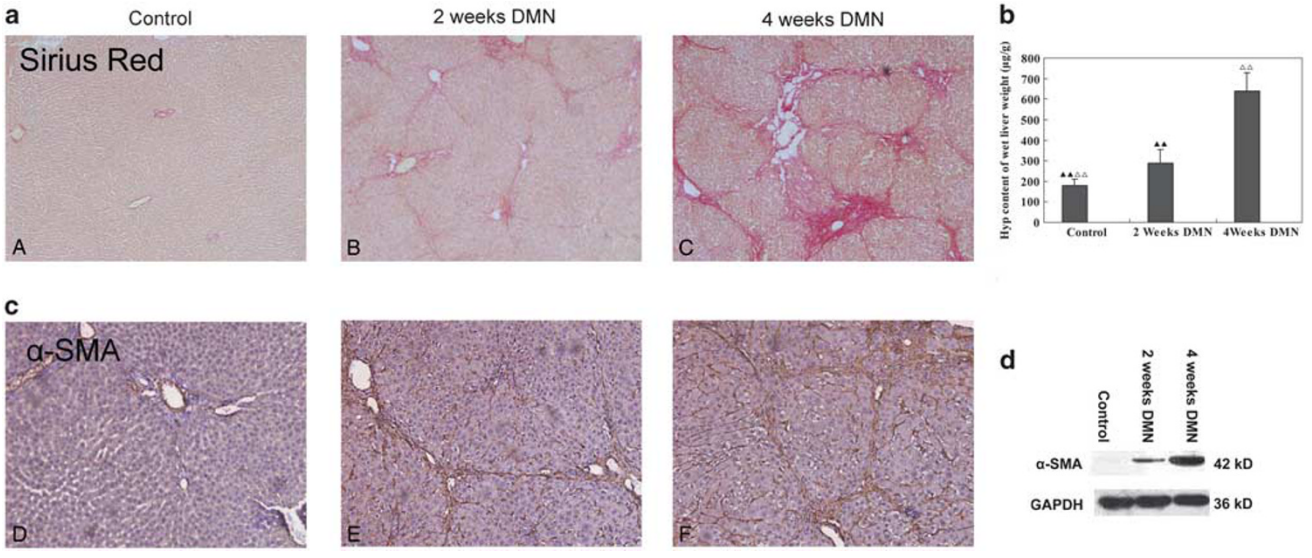

Figure 1 Chronic DMN treatment induced fibrosis after 2 and 4 weeks in rats. Rats were administrated with DMN for 2 or 4 weeks. (**a**) Liver sections were stained with Sirius red (A–C, × 100). (**b**) Hyp content of liver tissue was measured. The number in Hyp and sirus red detection was as the same as the animal number in each group. (**c**) Liver sections were stained with α-SMA antibody. Brown staining indicates immunopositivity (D–E, × 200, $n=4$). (**d**) Expression of α-SMA was analyzed using western blot ($n=6$). The data represented the mean ± s.d. $^{▲}P<0.05$, $^{▲▲}P<0.01$, *vs* 4-week DMN treatment; $^{Δ}P<0.05$, $^{ΔΔ}P<0.01$ *vs* 2-week DMN.

cirrhosis and accumulation of collagen bundles in 9-week CCL4-treatment rats shown in Supplementary Figure 1d.

As sustained deposition of extracellular matrix is mainly resulted from activation of HSC, a correlation between accumulated collagen and activated HSCs was studied by detecting a marker of activated HSC, α-SMA immunohistochemically in liver sections described above. In control rats, only vascular smooth muscle cells were strongly positive for α-SMA, whereas HSCs positive for α-SMA were rarely observed (Figure 1D; Supplementary Figure 1e). After 2 weeks of DMN or 6 weeks of CCL4 treatment, many α-SMA-positive HSCs were detected in areas of centrilobular and near periportal fibrotic bands (Figure 1E; Supplementary Figure 1f). The number of α-SMA-positive HSCs was even higher at 4-week DMN-treated or 9-week CCL4-treated cirrhotic livers (Figure 1F; Supplementary Figure 1g). The changed expression of α-SMA was also shown with a western blot (Figure 1d; Supplementary Figure 1h). Taken together, these results confirm that DMN and CCL4 administrations cause HSC activation and accumulation of extracellular matrix that might facilitate or result in liver fibrosis and cirrhosis.

Activation of KCs in Liver Fibrosis Reflected by Specific Markers of CD68 and TNF-α

Liver injury could associate with activation of KCs and trigger migration of macrophage into hepatic cords in which these macrophages stimulate fibrosis by secreting fibrogenic cytokines. To elucidate the functions of KCs in liver fibrosis, a specific KC marker, CD68, has been used to monitor KC activation.[8] As shown in Figure 2a and Supplementary Figure 2a, CD68-positive KCs were present in hepatic sinusoids and were at low levels in the control liver. After DMN and CCL4 administration, CD68-positive KCs with strong staining appeared not only in hepatic sinusoids, but also in portal areas and adjacent to fibrotic septa (Figure 2a). CD68-positive KCs with strong staining appeared mainly in the portal areas and fibrotic septa, but not in hepatic sinusoids in the 9-week CCL4 rats (Supplementary Figure 2c).

Consistent with the results of immunostaining of CD68 (Figure 2a), increased expression of CD68 was further confirmed with CD68 real-time PCR and a western blot (Figure 2b and c). Real-time PCR showed that CD68 transcript was up-regulated about 3.5-fold after 2 weeks of DMN treatment. Thereafter, mRNA expression declined slightly in the 4-week DMN-treated liver. Similar changes at the protein level of CD68 were observed in a western blot analysis (Figure 2c).

TNF-α is mainly derived from KCs after liver injury.[17] As presented in Figure 2b, in 2-week DMN-treated livers, the expression of TNF-α increased significantly ($P<0.01$) to more than fourfold compared with control as determined by a real-time PCR analysis. This increase of TNF-α expression, however, attenuated in 4-week DMN livers when compared

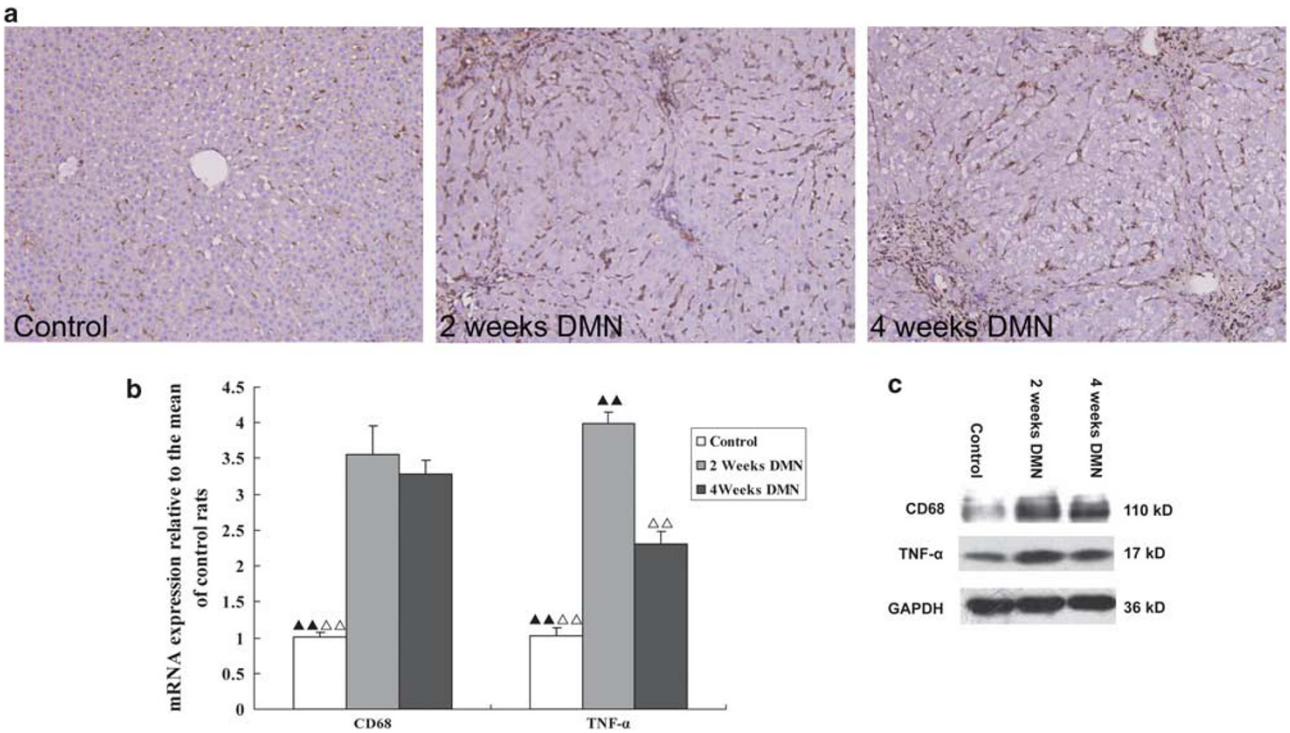

Figure 2 Dynamic changes of CD68 and TNF-α in DMN-induced liver fibrosis in rats. (**a**) CD68 was investigated by immunohistochemical analysis. Brown staining indicates immunopositivity. (× 200, $n=4$); (**b**) CD68 and TNF-α were measured by real-time PCR, as an internal control, 18S rRNA was amplified ($n=3$). (**c**) CD68 and TNF-α were detecting by western blot ($n=6$). The data represented the mean ± s.d. $^{▲}P<0.05$, $^{▲▲}P<0.01$, *vs* 4-week DMN treatment; $^{△}P<0.05$, $^{△△}P<0.01$ *vs* 2-week DMN treatment.

with 2-week DMN livers ($P<0.01$). The expression of TNF-α was further confirmed by a western blot (Figure 2c). The expressions of CD68 and TNF-α were increased gradually after CCL4 treatment (Supplementary Figure 2d). These results suggest that more KCs were migrated into hepatic lobules in liver injury and are consistent with the notion that KC is a major source of TNF-α production.[14]

Apoptotic CD68-Positive KCs Were Observed in Liver Fibrosis

It is generally believed that during liver fibrosis, KCs engulf apoptotic cells of various cell types including hepatocytes, neutrophils, and erythrocytes.[14–16] Less attention was paid to a possibility of existence of apoptotic KCs in fibrotic livers. Here, by using laser confocal microscopy, we revealed that

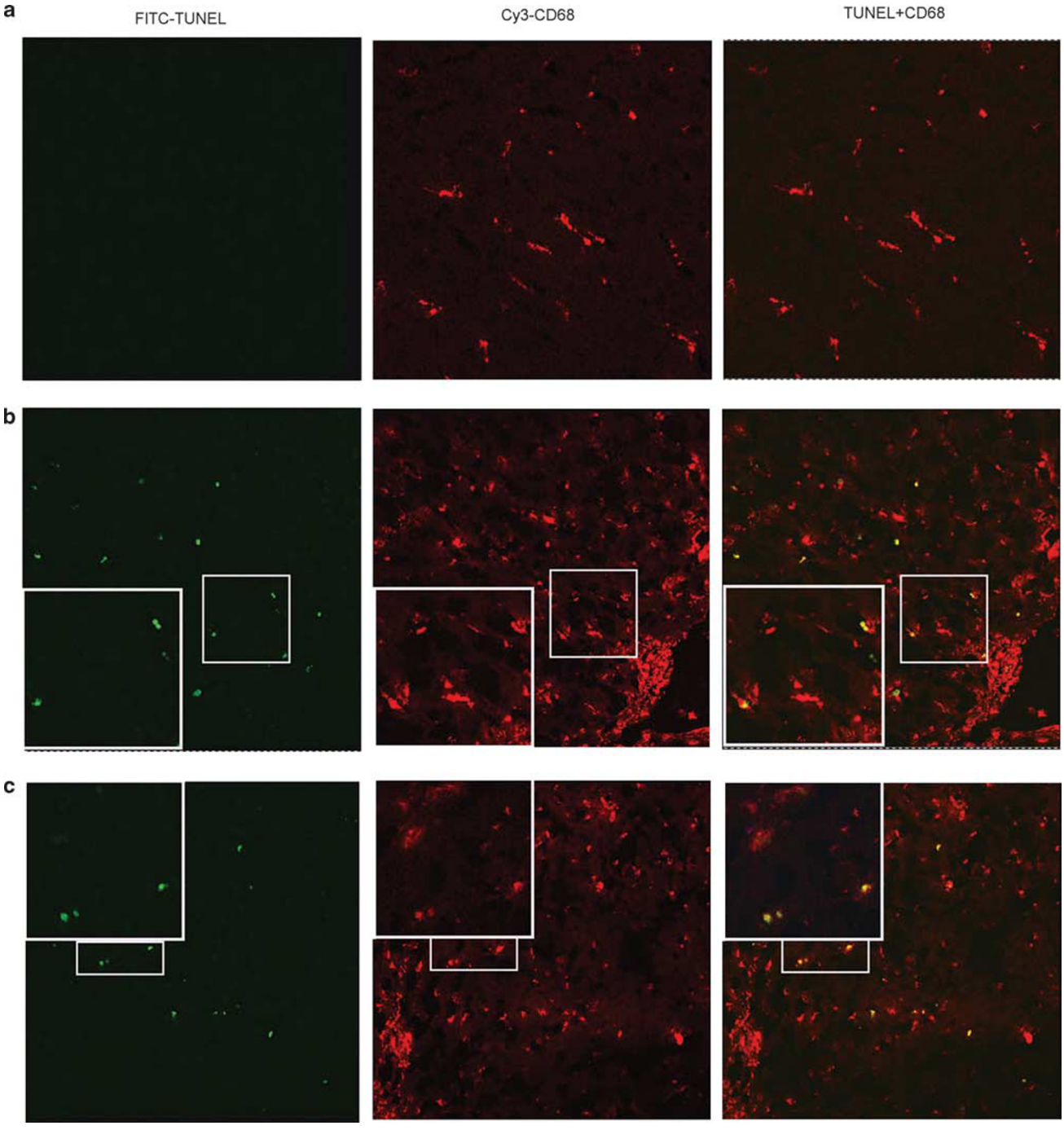

Figure 3 KC apoptosis was detected using confocal microscopy in DMN-induced liver fibrosis in rats. Hepatic cryosections stained with TUNEL (green) and CD68 (red); (**a**) control; (**b**) 2-week DMN treatment; and (**c**) 4-week DMN treatment. The yellow color denotes co-localization (× 400, $n=4$). The boxed area in the slide was enlarged and shown in the inset (× 600).

KCs could undergo apoptosis in DMN (Figure 3) and CCL4 (Supplementary Figure 3)-induced liver fibrosis. Apoptotic KCs shown as double positive for TUNEL and CD68 were rarely observed in a control liver (Figure 3a). After 2 weeks of DMN administration, number of cells with co-staining signals of TUNEL and CD68 increased markedly. These TUNEL-, CD68-double-positive KCs decreased apparently in 4-week DMN liver compared with 2-week DMN liver (Figure 3b and c).

To show directly that KCs undergo apoptosis in fibrotic livers, we isolated KCs from both normal and DMN-caused fibrotic livers with a method that preferentially enriches KCs with a $>95\%$ purity in a preparation. After 6 h culture, cells attached to the culture dishes were fixed and immunostained for the detection of apoptotic KCs. As shown in Supplementary Figure 4, TUNEL and CD68-double-positive cells were easily observed in the photos of a confocal microscope in cultured cells that were isolated from fibrotic livers. As TUNEL and CD68 staining are specific markers for apoptotic cells and KCs, respectively, co-localization of both signals on the same cells suggest a possibility that these KCs isolated from fibrotic livers were in the process of apoptosis.

In contrast, CD68 and TUNEL-double-positive cells were rarely, if any, observed in cultured KCs isolated from normal livers. As experimental conditions of isolation and culturing of KCs were the same for both normal and DMN-treated livers, the reason of appearance of apoptotic KCs in this *in vitro* system can be attributed to livers that were damaged by DMN administrations.

Fas-Mediated CD68-Positive KC Apoptosis

The Fas/FasL death pathway is involved in various forms of physiological and pathological cell death.[24] In this study, we also investigated whether Fas mediated KC apoptosis in liver fibrosis. As shown by serial sections in Figure 4, Fas-positive cells were mainly located in hepatic sinusoids in the DMN-treated rats (Figure 4a and d), CD68-positive KCs were also found in the sinusoid (Figure 4b and e), and occupied the same space as Fas-positive cells. Meanwhile, laser confocal microscopy showed that Fas was co-localized with TUNEL (data not shown), suggesting that Fas might mediate KC apoptosis in liver fibrosis.

Co-localization of TUNEL, CD68, and α-SMA in Liver Fibrosis

To elucidate pathophysiological involvement of apoptotic and activated KCs in DMN and CCL4-induced liver fibrosis, co-localization status among TUNEL, CD68, and α-SMA was studied using confocal microscopy.

As shown in Figure 5 b and f, although some TUNEL-positive cells were distributed closely to α-SMA-positive-HSCs, co-localization of TUNEL and α-SMA was scarcely observed in 2- or 4-week DMN livers. This result was consistent with our earlier reports: α-SMA-positive-HSCs did not co-localize with TUNEL-positive cells in DMN-induced liver fibrosis.[20] Co-localization of TUNEL and α-SMA was also scarcely observed in 6- or 9-week CCL4 rats (Supplementary Figure 5). TUNEL and CD68-double-positive apoptotic KCs (Figure 5a and e) laid closely adjacent to $\alpha\text{-SMA}^+$ HSCs (Figure 5d and h). These results were also

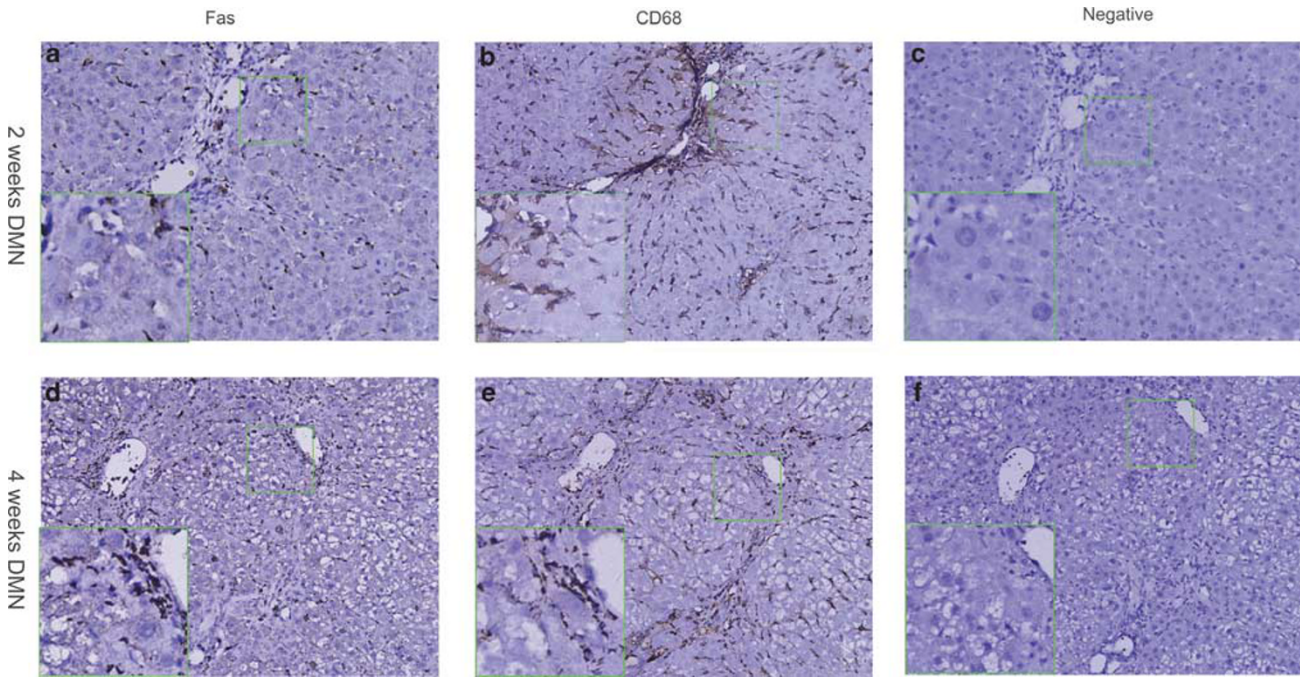

Figure 4 Co-existence of Fas (**a**, **d**) and CD68 (**b**, **e**) was determined by immunohistochemistry using serial sections stained with different antibodies ($\times 200$). Negative control (**c**, **f**) showed no antibody. The boxed area in each slide was enlarged and shown in the left inset ($n=4$) ($\times 400$).

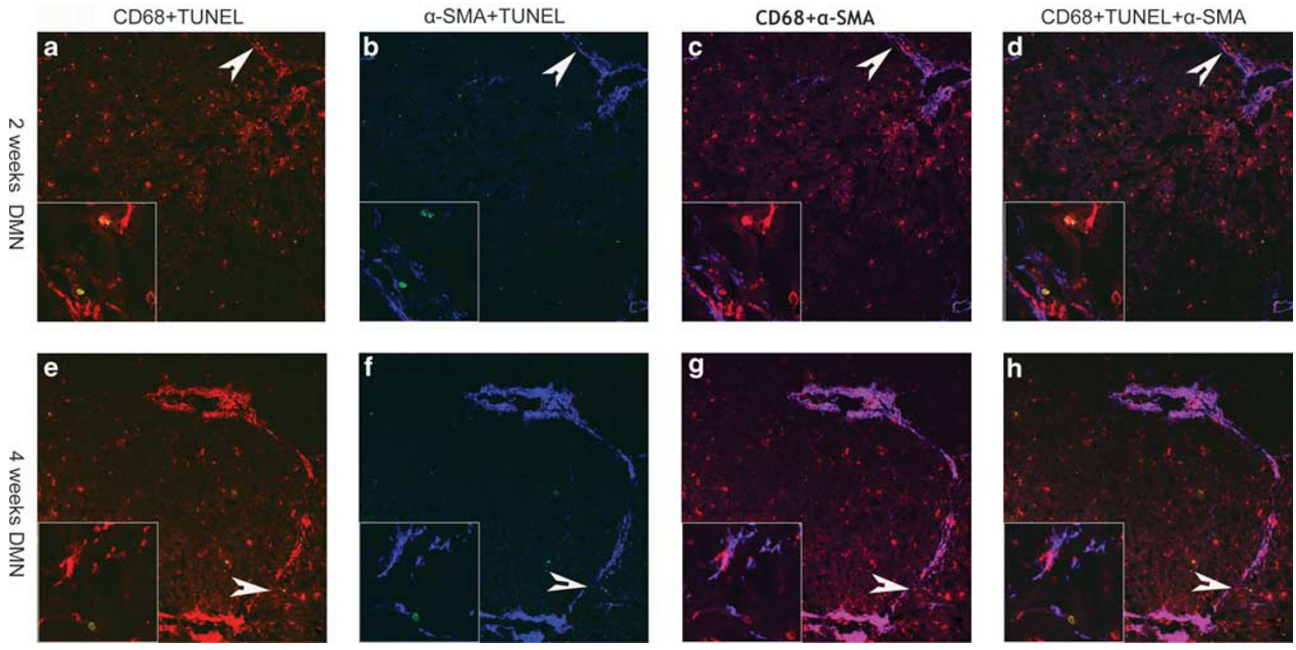

Figure 5 Hepatic cryosections were stained using tri-color immunofluorescence staining consisting of TUNEL (green), CD68 (red), and α-SMA (blue) to determine the relationship between HSCs and activated or apoptotic KCs (× 200). Arrowheads point to apoptotic KCs and is enlarged in boxed area in each image ($n = 4$) (× 600). (**a**) Co-localization of TUNEL, CD68 was observed in 2-week DMN liver. (**b**) Double TUNEL$^+$α-SMA$^+$HSCs was not observed. (**c**) Co-existence of CD68 and α-SMA were clearly observed indicating interaction between KCs and HSCs. (**d**) Apoptotic KCs laid adjacent to α-SMA$^+$ HSCs in the fibrotic septa or portal areas. The same phenomenon was observed in (**e**–**h**).

shown in CCL4-treated liver, indicating that those apoptotic KCs might be involved in HSC activation in liver fibrosis.

As shown in Figure 5c, CD68$^+$ KCs located closely or attached directly to α-SMA$^+$ HSCs in portal area in 2-week DMN liver. In 4-week DMN liver or 9-week CCL4 liver, rampant adhesion of KCs and HSCs was observed in thick fibrotic bands in sinusoid and portal area (Figure 5g; Supplementary Figure 5).

These results showed that (1) some KCs undergo apoptosis in liver fibrosis; (2) α-SMA-positive HSCs are not apoptotic cells as others have earlier reported;[25,26] and (3) the interaction between KCs and HSCs becomes more and more rampant during liver fibrosis development in DMN- and CCL4-treated rats.

Co-localization of CD68, TNF-α, and α-SMA in Liver Fibrosis

It has been well known that TNF-α, a proinflammatory cytokine, has an important function in the pathogenesis of liver fibrosis, and KCs are the primary source of this cytokine.[17,27] However, there was little evidence to support that TNF-α was derived from KCs *in vivo*. As shown in Figure 6 and Supplementary Figure 6, we provided clear evidence that TNF-α was produced from KCs *in vivo*. In control rats, double positive of CD68 and TNF-α cells were separated from α-SMA-positive cells, indicating that there was minimal interaction between TNF-α derived from KCs and HSCs (Figure 6d). After 2 weeks of DMN treatment or 6 weeks of CCL4 treatment, numbers of CD68-positive KCs, TNF-α-positive cells, and α-SMA-positive HSCs were significantly increased in hepatic lobules compared with control livers (Figure 6; Supplementary Figure 6). Cells of double positive of CD68 and TNF-α (Figure 6e and h) were easily found in lobules, especially in incomplete septa (Figure 6e). This result directly showed that a portion of KCs migrated into hepatic lobules and generated TNF-α in DMN- and CCL4-treated rats. More interestingly, those TNF-α producing KCs were located closely to activated HSCs (Figure 6g and h). After 4 weeks of DMN treatment, the number of TNF-α and CD68-double-positive cells decreased and the expression level of TNF-α in individual-positive cells declined when compared with sections of 2-week DMN liver (Figure 6i and l). On the other hand, α-SMA-positive cells at this time point became more predominant that might be responsible for exaggerative pathological changes in liver (Figure 6k and l). The number of TNF-α, CD68, and α-SMA-triple-positive cells increased gradually after CCL4 administration (Supplementary Figure 6). These results showed that the activated KCs stimulate HSCs' activation through TNF-α.

Co-localization of CD68, Col (1), and α-SMA in Liver Fibrosis

Col (1) is mainly derived from activated HSCs, whereas it is rarely reported to be secreted by CD68-positive cells. As shown in Figure 7 and Supplementary Figure 7, in the portal triads of normal liver, the hepatic central vein wall stains

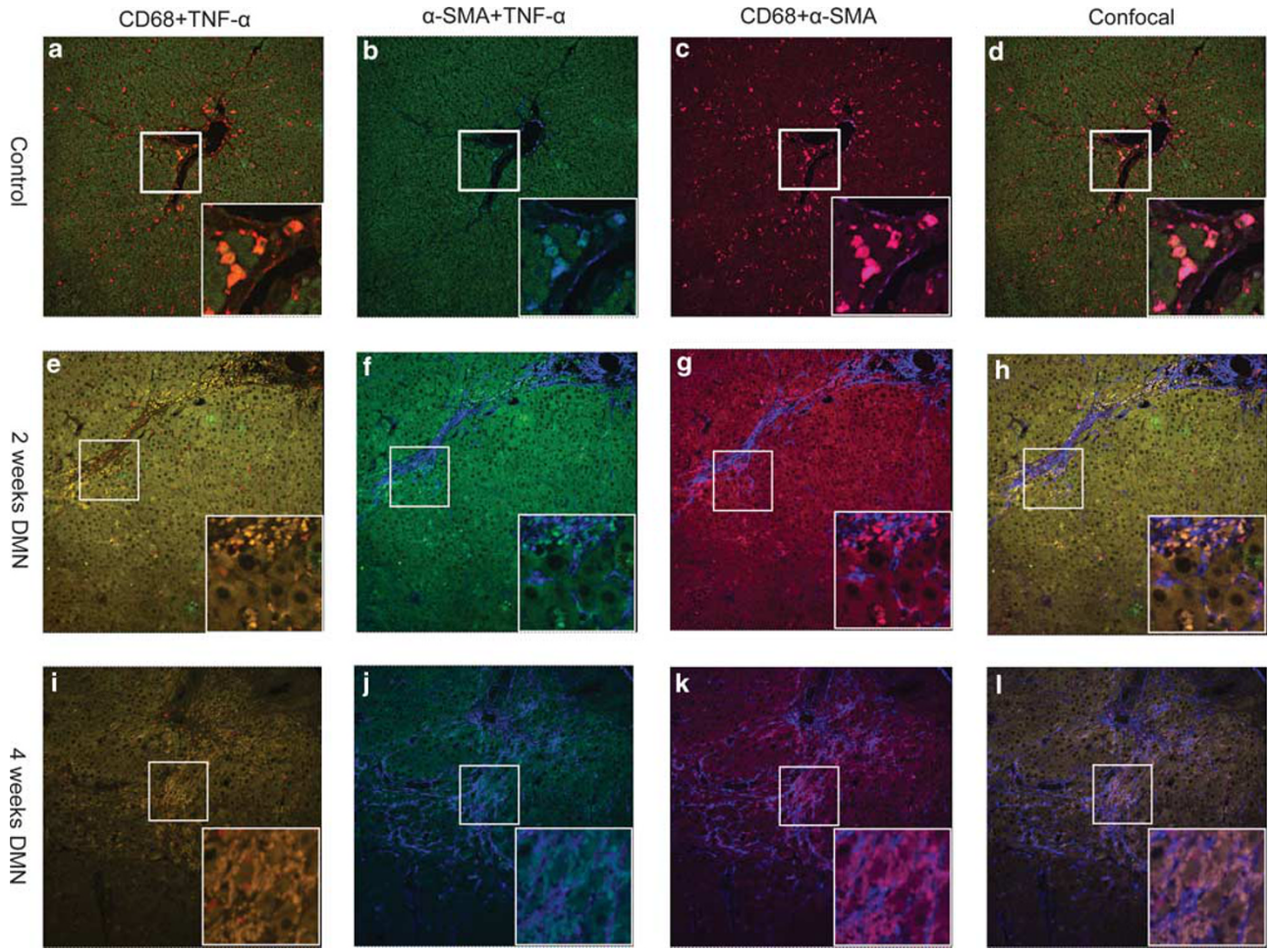

Figure 6 Confocal microscopy of conducting serial liver sections in control (**a–d**), 2-week DMN (**e–h**) and 4-week DMN (**i–l**) in rats is shown. TNF-α derived from KCs participated in stimulating HSC activation in DMN-induced liver fibrosis in rats. Hepatic paraffin sections were CD68 (red), TNF-α (green) and α-SMA (blue) (× 200). The boxed area in each image is enlarged and shown in the insets ($n = 4$) (× 600).

positively for α-SMA and Col (1), whereas the CD68-positive cells and their surrounding area were almost negative for Col (1) (Figure 7a–d). The staining for α-SMA and Col (1) was remarkably increased and distributed in parallel in DMN-treated livers, especially in the 4-week DMN livers (Figure 7e and i), consistent with the notion that activated HSCs are a major resource of Col (1) production in liver fibrosis. Surprisingly, when sections were stained with CD68 and Col (1) antibodies, some CD68 and Col (1) double positive, but completely negative for α-SMA, were found in the portal areas and hepatic sinusoids (Figure 7f and h), suggesting a possibility that KCs might participate in the Col (1) production during livers fibrosis. Similar results were also found in the livers of CCL4-treated rats (Figure 7i–l; Supplementary Figure 7).

To show directly that KCs could produce collagen, an *in vitro* culture system was established for KCs that were isolated from either normal or DMN-caused fibrotic livers. KCs from normal livers were Col (1) negative after 48 h culture in the absence of LPS (Figure 8). LPS treatment at a concentration of 100 μg/l for 6 h, however, could result in weak Col (1) staining in isolated KC cells. Higher magnification images clearly showed that the Col (1)-positive cells were all CD68-positive cells in tri-color confocal microscopy. Absence of α-SMA and Col (1)-double-positive cells in culture indicated that these Col (1)-positive cells were not contaminating HSCs. Col (1) and CD68-double-positive KCs were clearly detected in cultured KCs isolated from fibrotic livers even without an earlier LPS stimulation. After LPS stimulation, Col (1) staining of KCs isolated from fibrotic livers was more intensive when compared with the staining of KCs that were isolated from a normal liver.

Col (1) expression in KCs was further verified with Col 1(α1) mRNA analysis of isolated KCs. As shown in Supplementary Figure 7, Col 1(α1) mRNA expression in KCs isolated from fibrotic rats was significantly higher than that of KCs isolated from control rats, even control KCs were stimulated with LPS. The mRNA level of collagen α1(I) in LPS-treated KCs was increased significantly ($P < 0.05$) when compared with LPS-untreated KCs (Supplementary Figure 8).

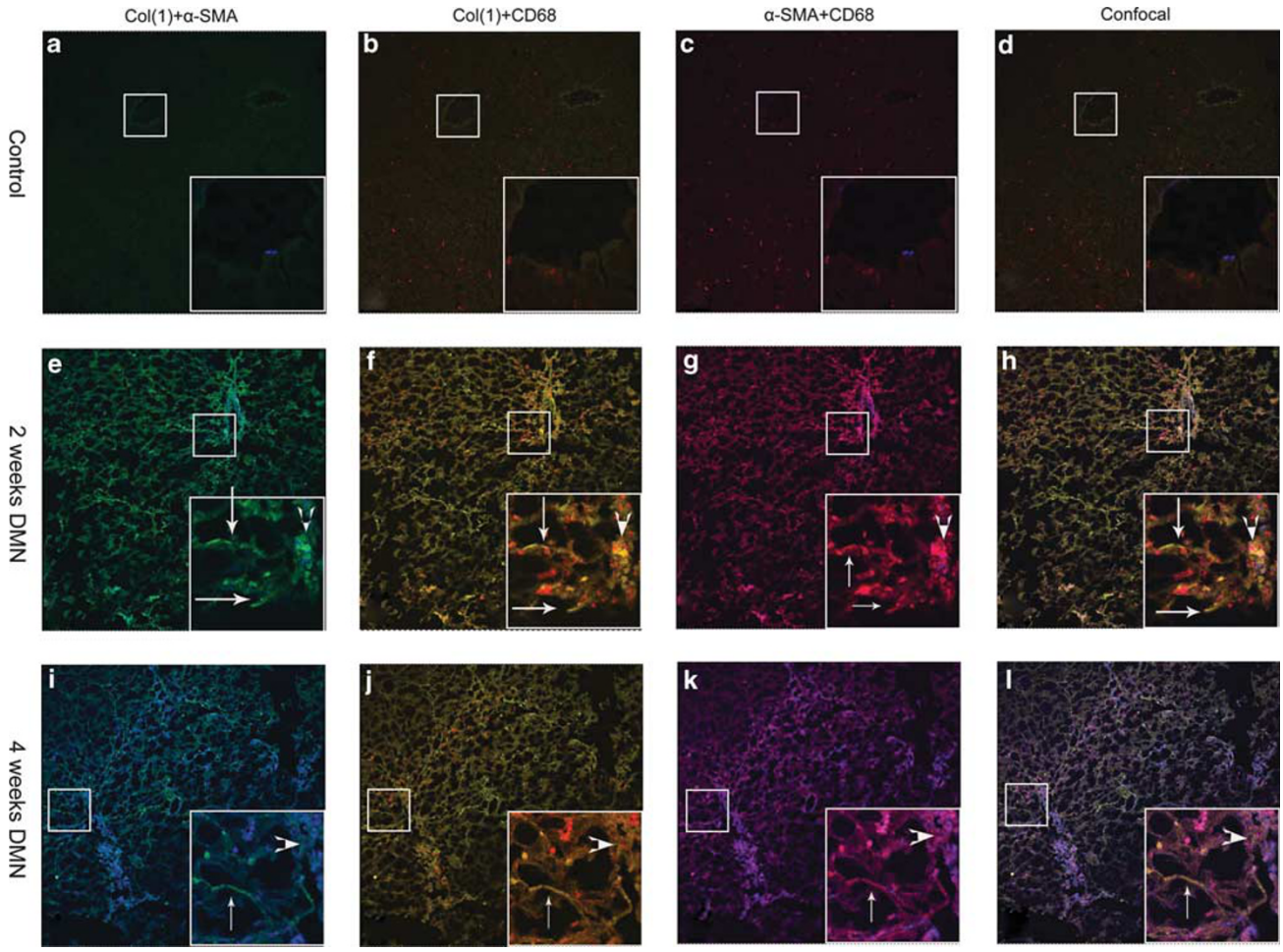

Figure 7 Confocal microscopy of conducting serial liver sections in control (**a–d**), 2-week DMN (**e–h**) and 4-week DMN (**i–l**) in rats is shown. Hepatic cryosections were stained with Col (1) (green), CD68 (red) and α-SMA (blue) (× 200). The arrow indicates Col (1) derived from KCs only. The arrowhead indicates Col (1) derived from the interaction between KCs and HSCs. The boxed area in each image is enlarged and shown in the insets ($n = 4$) (× 600).

Taken together, KCs in DMN-treated rats produced collagen that might have an important function in the development of liver fibrosis in rats.

DISCUSSION

Liver fibrosis is a complicated pathological process in which multiple components including KCs, HSCs, hepatocytes, and various cytokines and fibrotic matrix proteins are actively participated. Currently, extensive studies are aimed to establish a mechanistic link between hepatocellular apoptosis, inflammation, and fibrosis in chronic liver diseases.[13,14] There is overwhelming evidence that activated HSCs are the major producers of the fibrotic matrix and that HSC apoptosis is the primary mechanism of regression of liver fibrosis.[25,28] Inflammation is the main characteristic in liver fibrosis and KCs are considered to be the primary source of inflammatory cytokines.[17] In this study, using confocal microscopy, we revealed several KCs-related phenomena in the livers of DMN- and CCL4-treated rats that were not reported earlier.

It has been well known that KCs engulf apoptotic cells in liver injury,[14–16] but KC apoptosis by itself has been largely ignored and rarely reported. In contrast to others studies, our results provide the ample evidences that KCs undergo apoptosis in liver fibrosis *in vivo* (Figures 3 and 5; Supplementary Figure 3, 4, and 5). First, co-staining of CD68, a KC-specific marker, and TUNEL characteristic for apoptotic cells strongly suggest that these cells were apoptotic KCs, rather than KCs engulfing some apoptotic bodies of hepatocytes or neutrophils in response to liver injury, as phagocytosis by KCs such as CD68-positive cells (ED1 cells) was barely detectable.[29] Second, Fas-positive cells were found almost in hepatic sinusoids (Figure 4), in which CD68 was detected. This co-localization of Fas-positive cells, CD68, and TUNEL-double-positive KCs was consistent with a scenario that Fas, through Fas receptor pathway, medicates apoptosis of those KCs. However, based on our knowledge, it was rarely reported that Fas mediates KC apoptosis in liver fibrosis *in vivo*.

It has been claimed that HSCs undergo apoptosis during the regression of liver fibrosis.[25,28] It is interesting to observe

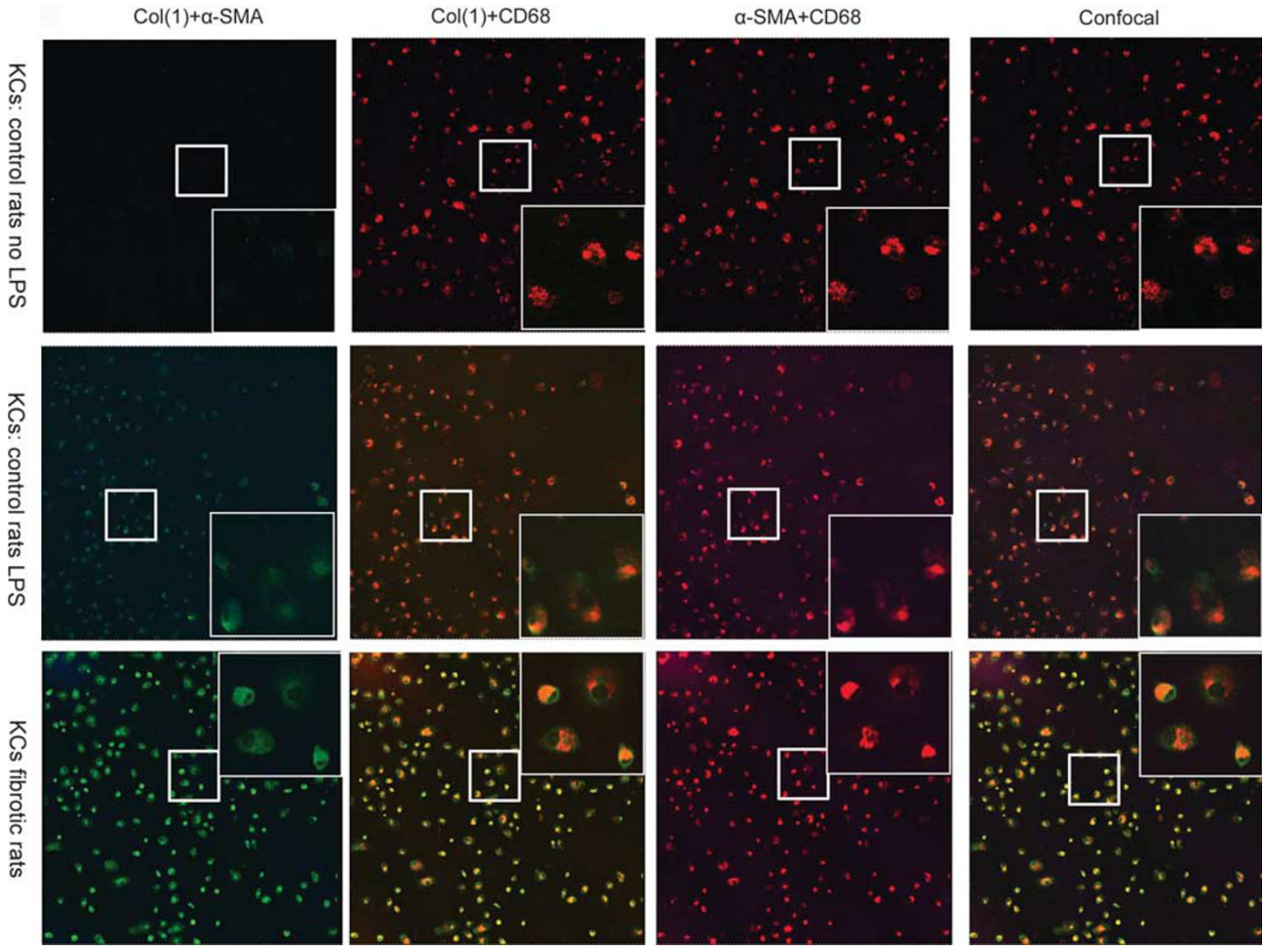

Figure 8 Co-localization of CD68, Col (1), and α-SMA was examined in primary KCs *in vitro*. Kupffer cells isolated from control were cultured 48 h, then with 100 μg/l LPS for 6 h. After purification, the freshly KCs isolated from fibrotic rats were used for confocal microscopy. The cells were stained with Col (1) (green), CD68 (red), and α-SMA (blue) (× 200). The boxed area in each image is enlarged and shown in the insets (× 600) ($n = 3$).

that the α-SMA-positive HSCs in the portal areas and fibrotic septa were free of TUNEL staining. Consistent with our earlier report,[20] this finding is not unexpected and we believe that the following factors might make a contribution to this result. First of all, in the livers treated with 2-week DMN, there was already a peak in the level of apoptotic cells, whereas HSC activation, shown as α-SMA-positive cells, has just begun to be activated. Second, our model was studying liver fibrosis rather than liver repair and regression, in which more apoptotic HSCs exist. As shown in tri-color staining of TUNEL, CD68, and α-SMA, apoptotic KCs in the portal areas were close to the α-SMA-positive HSCs in both DMN- and CCL4-treated livers, suggesting a direct interaction between apoptotic KCs and activated HSCs in the fibrotic septa of those liver samples.

KCs could activate HSCs by producing and releasing a variety of mediators, such as proinflammatory cytokines and reactive oxygen species that fulfill a crucial function in the inflammatory responses of the liver.[30] Several studies have evaluated the function of KCs in stimulating HSCs using conditioned medium.[31] KCs generate ROS and IL-6, which in turn enhance HSC activation.[16] Recently, researchers have shown that TGF-β1 derived from KCs promotes the activation of TLR-4-MyD88-NF-κB-dependent HSCs that is subsequently responsible for the paracrine fibrogenesis in liver.[31] These *in vitro* approaches, however, might not reflect the true microenvironmental interactions of KCs and HSCs *in vivo*. To overcome these obstacles, we developed a laser confocal system to characterize the intercellular communication between KCs and HSCs and to better understand the mechanisms by which KCs-derived mediators induce a fibrogenic response in HSCs. Consistent with earlier studies, it was confirmed in this study that KCs secreted the proinflammatory mediators such as TNF-α after DMN and CCL4 treatment. Moreover, double positive of TNF-α and CD68 cells were closely adjacent to HSCs, indicating that activated CD68-positive KCs might stimulate HSCs through TNF-α pathway.

Another major aim of this study was to assess whether HSC activation by KCs can lead to the production of Col (1), a major component of pathological ECM, or if KCs can produce Col (1) independently in liver fibrosis in rats. To address this issue, the co-localization of CD68, α-SMA, and Col (1) in liver was studied with confocal system. As expected, double α-SMA and Col (1)-positive cells predominantly existed in fibrotic septa. Those cells were co-localized clearly with CD68-positive cells, indicating that activated HSCs are the main resource of Col (1) production, probably through KCs-mediated stimulation or some direct interaction of these two types of cells. Surprisingly, we also observed the presence of double CD68 and Col (1)-positive cells in these sections. Some of them were separated from α-SMA-positive HSCs, suggesting KCs themselves might have fibrogenic ability by producing Col (1) independently in this *in vivo* model.

In summary, the major findings of this study include (1) some CD68-positive KCs in DMN-caused fibrotic livers undergo apoptosis; (2) TNF-α produced from KCs might actively participate in the activation of HSCs; and (3) Col (1) was predominantly produced from HSCs as a result of the interactions between HSCs and KCs and also could be derived from KCs, independently, in the liver of DMN- and CCL4-treated rats. These data not only benefit our understanding of the mechanism of hepatic fibrosis, but also suggest potentially therapeutical manipulations of suppressing proinflammatory KCs for the attenuation of liver fibrosis.

Supplementary Information accompanies the paper on the Laboratory Investigation website (http://www.laboratoryinvestigation.org)

ACKNOWLEDGEMENTS

We thank Dr Wuxiong Zhou (Basic Colloge of Traditional Chinese Medicine) for technical support with laser confocal microscopy. This work was mainly supported by The National Natural Science Foundation of China (No. 90409020, 30701070), National Basic Research Program of China (2006CB504800), Innovative Research Team in Universities, Shanghai Municipal Education Commission, Key Laboratory of Liver and Kidney Diseases (Shanghai University of Chinese Medicine), The Ministry of Education, E-institute of Shanghai Municipal Education Commission (No.03008), and The China Postdoctor Foundation (No. 20090450726).

DISCLOSURE/CONFLICT OF INTEREST

The authors declare no conflict of interest.

1. Iredale JP. Models of liver fibrosis: exploring the dynamic nature of inflammation and repair in a solid organ. J Clin Invest 2007;117:539–548.
2. Friedman SL. Mechanism of hepatic liver fibrosis. Gastroenterology 2008;134:1655–1669.
3. Iredale JP. Defining the therapeutic targets for liver fibrosis: exploiting the biology of inflammation and repair. Pharmcol Res 2008;58:129–136.
4. Friedman SL, Don C, Rockey DC, *et al.* Hepatic fibrosis 2006: report of the Third AASLD Single Topic Conference. Hepatology 2007;45: 242–249.
5. De Minicis S, Seki E, Uchinami H, *et al.* Gene expression profiles during hepatic stellate cell activation in culture and *in vivo*. Gastroenterology 2007;132:1937–1946.
6. Duffield JS, Forbes SJ, Constandinou CM, *et al.* Selective depletion of macrophages reveals distinct, opposing roles during liver injury and repair. J Clin Invest 2005;115:56–65.
7. Friedman SL. Mac the knife? Macrophages-the double-edged sword of hepatic fibrosis. J Clin Invest 2005;115:29–32.
8. Fallowfield JA, Mizuno M, Kendall TJ, *et al.* Scar-associated macrophages are a major source of hepatic matrix metalloproteinase-13 and facilitate the resolution of murine hepatic fibrosis. J Clin Invest 2007;178:5288–5295.
9. Kendall TJ, Hennedige S, Aucott RL, *et al.* p75 neurotrophin receptor signaling regulates hepatic myofibroblast proliferation and apoptosis in recovery from rodent liver fibrosis. Heptology 2009;49:901–910.
10. Gehring S, Dickson EM, Martin MES, *et al.* Kupffer cells abrogate cholestatic liver injury in mice. Gastroenterology 2006;130:810–822.
11. Friedman SL. Molecular regulation of hepatic fibrosis, an integrated cellular response to tissue injury. J Biol Chem 2000;275:2247–2250.
12. Galle PR. Apoptosis in liver disease. J Hepatol 1997;27:405–412.
13. Canbay A, Friedman SL, Gores GJ. Apoptosis: the nexus of liver injury and fibrosis. Hepatology 2004;39:273–278.
14. Canbay A, Feldstein AE, Higuchi H, *et al.* Kupffer cells engulment of apoptotic bodies stimulates death ligand and cytokine expression. Hepatology 2003;38:1188–1198.
15. Shi J, Fujieda H, Kokubo Y, *et al.* Apoptosis of neutrophils and their elimination by Kupffer Cells in rat liver. Hepatology 1996;24:1256–1263.
16. Otogawa K, Kinoshita K, Fujii H, *et al.* Erythrophagocytosis by liver macrophages (Kupffer cells) promotes oxidative stress, inflammation, and fibrosis in a rabbit model of steatohepatitis. Am J Pathol 2007;170:967–980.
17. Nieto N. Oxidative-stress and IL-6 mediate the fibrogenic effects of rodent kupffer cells on stellate cells. Hepatology 2006;44:1487–1501.
18. Imamura M, Ogara T, Sasaguri Y, *et al.* Suppression of macrophage infiltration inhibits activation of hepatic stellate cells and liver fibrogensesis in rats. Gastroenterology 2006;128:138–146.
19. Tekehara T, Hayashi N, Mita E, *et al.* Delayed Fas-mediated hepatocyte apoptosis during liver regeneration in mice, hepatoprotective role of TNF-α. Hepatology 1998;27:1643–1651.
20. Liu C, Sun M, Yan X, *et al.* Inhibition of hepatic stellate cells activation following the administration of Yin-chen-hao decoction to dimethylnitrosamine treated rats. Hepatol Res 2008;38:919–929.
21. Ala-Kokko L, Pihlajaniemi T, Myers JC, *et al.* Gene expression of type III I and IV collagens in hepatic fibrosis induced by dimethylnitrosamine in the rat. Biochem J 1987;244:75–79.
22. Nakamura T, Akiyoshi H, Saito I, *et al.* Adenovirus-mediated gene expression in the septal cells of cirrhotic rat livers. J Hepatol 1999;30:101–106.
23. Jamall IS, Finelli VN, Que Hee SS. A simple method to determine nanogram levels of 4-hydroyproline in biological tissues. Anal Biochem 1981;112:70–75.
24. Ku N, Soetikno RM, Omary MB. Keratin mutation in transgenic mice predisposes to Fas but not TNF-induced apoptosis and massive liver injury. Hepatology 2003;37:1006–1014.
25. Kweon YO, Paik YH, Schnabl B, *et al.* Gliotoxin-mediated apoptosis of activated human hepatic stellate cells. J Hepatol 2003;39:38–46.
26. Aana A, Baskin-Bey ES, Bronk SF, *et al.* Proteasome inhibitors induce hepatic stellate cell apoptosis. Hepatology 2006;43:335–342.
27. Uchimura K, Nakamuta M, Enjoji M, *et al.* Activation of retinoic X receptor and peroxisome proliferator-activated receptor-g inhibits nitric oxide and tumor necrosis factor-α production in rat Kupffer Cells. Hepatology 2001;33:91–99.
28. Burt AD. Cellular and molecular aspects of hepatic fibrosis. J Pathol 1993;170:105–114.
29. Gomes LF, Lorente S, Simon-Giavarotti KA, *et al.* Triiodothyronine differentially induces Kupffer cell ED1/ED2 subpopulations. Mol Aspects Med 2004;25:183–190.
30. Tomita K, Tamiya G, Ando S, *et al.* Tumor necrosis factor alpha signalling through activation of Kupffer cells plays an essential role in liver fibrosis of non-alcoholic steatohepatitis in mice. Gut 2006;55:415–424.
31. Seki E, De Minicis S, Osterreicher CH, *et al.* TLR4 enhances TGF-β signaling and hepatic fibrosis. Nat Med 2007;11:1324–1332.